polymers described here, poly(m^6-GMP) and poly(e^6-GMP).

The spectra studies shown in Figures 1 and 2 and in Table II indicate that these polymers possess a secondary structure with a high degree of hypochromicity. Poly(e^6-GMP) has consistently more hypochromicity than poly(m^6-GMP), and probably represents an exaggeration of its secondary structure.

The curves shown in Figure 5 demonstrate cooperative melting behavior for both poly(m^6-GMP) and poly(e^6-GMP), in marked contrast to the very slight and very gradual increase in optical density shown by poly(G) under these conditions.

Although both analogue polymers depurinate slowly under strongly acid conditions, we were able to obtain reversible melting curves at pH 3. The melting profiles at pH 3, 5, and 7 are all similar, but melting temperature increases as pH is lowered. The melting point is higher at all pH's for poly(m^6-GMP) than for poly(e^6-GMP), indicating that the former polymer has a more stable structure. As pH is lowered below 3, an acid transition is evidenced by precipitation of the polymer.

The biological effects of methylation and ethylation are frequently rather different. The data presented here, however, indicate only quantitative differences in physical properties resulting from methylation vs. ethylation of the O^6 position of guanine. Observed differences in biological effects may reflect these quantitative differences or, more likely, result from differences in the sites and extent of methylation and ethylation.

In summary, the evidence presented here indicates that either methylation or ethylation of the O^6 position of guanine changes its normal base-pairing properties. Polymers of these analogue nucleotides, poly(m^6-GMP) and poly(e^6-GMP), have an ordered structure that exhibits cooperative melting; additional studies are in progress to further elucidate this secondary structure.

References

Craddock, V. M. (1973), *Biochim. Biophys. Acta 312,* 202.

Gerchman, L. L., Dombrowski, J., and Ludlum, D. B. (1972), *Biochim. Biophys. Acta 272,* 672.

Gerchman, L. L., and Ludlum, D. B. (1973), *Biochim. Biophys. Acta 308,* 310.

Kleihues, P., and Magee, P. N. (1973), *J. Neurochem. 20,* 595.

Lawley, P. D. (1972), *Top. Chem. Carcinog., Proc. Int. Symp., 2nd, 1971* 237–258.

Lawley, P. D., and Thatcher, C. J. (1970), *Biochem. J. 116,* 693.

Loveless, A. (1969), *Nature (London) 223,* 206.

Ludlum, D. B. (1970), *J. Biol. Chem. 245,* 477.

Ludlum, D. B. (1975), *Handb. Exp. Pharmakol., Part 2, 38,* 6–17.

Ludlum, D. B., and Wilhelm, R. C. (1968), *J. Biol. Chem. 243,* 2750.

O'Connor, P. J., Capps, M. J., and Craig, A. W. (1973), *Br. J. Cancer 27,* 153.

Sarma, D. S. R., Rajalakshmi, S., and Farber, E. (1975), in Cancer, Vol. 1, Becker, F. F., Ed., New York, N.Y., Plenum Press, pp 235–287.

Singer, B. (1972), *Biochemistry 11,* 3939.

Singer, B. (1975), *Prog. Nucleic Acid Res. Mol. Biol. 15,* 219–331.

Singer, B., and Fraenkel-Conrat, H. (1970), *Biochemistry 9,* 3694.

Vinograd, J., Bruner, R., Kent, R., and Weigle, J. (1963), *Proc. Natl. Acad. Sci. U.S.A. 49,* 902.

Conformation of the Extracellular Polysaccharide of *Xanthomonas campestris*†

G. Holzwarth

ABSTRACT: The solution conformation of the extracellular polysaccharide of the bacterium *Xanthomonas campestris* is examined by optical rotation, viscometry, and potentiometric titration. Measurements of optical rotation vs. temperature for solutions of the polysaccharide at low ionic strength reveal a sharp transition to a denatured structure which is reversible if sufficient salt is present. The temperature T_m at the transition midpoint increases as log (Na^+) or log (Ca^{2+}). Viscosity–temperature profiles substantiate a structural change of the polysaccharide at T_m. The intrinsic viscosity of the native molecule at zero shear rate exceeds 5000 ml/g. This high figure is indicative of a stiff chain. The viscosity of the native molecule is relatively insensitive to salt, whereas the denatured molecule collapses if salt is present. Hydrogen-ion titration shows that the pK_{app} of the COO^- groups of the polymer decreases from 3.2 in 0.01 M NaCl to 2.6 in 0.2 M NaCl. All these data suggest that the native polysaccharide possesses ordered secondary structure stabilized by nonionic interactions outweighing the repulsion between adjacent COO^- groups.

The bacterium *Xanthomonas campestris* produces an anionic extracellular polysaccharide which normally provides the organism with a protective slime. The polysaccharide appears to be essential to the pathogenicity of the organism toward its plant host, presumably by blocking the flow of fluids through the xylem (Sutton and Williams, 1970). When grown on a glucose-containing medium in a fermentor, the bacterium produces large amounts of the extracellular polymer (Jeanes

† From the Corporate Research Laboratories, Exxon Research and Engineering Co., Linden, New Jersey 07036. *Received March 29, 1976.*

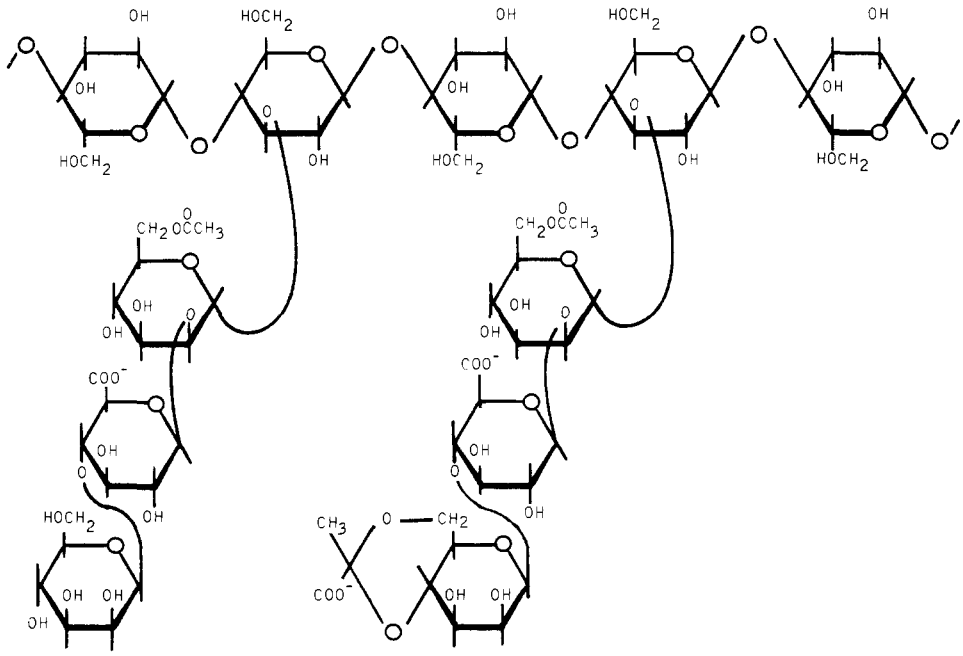

FIGURE 1: Structure of extracellular polysaccharide of *Xanthomonas campestris*, according to Jansson et al. (1975).

et al., 1961). It is convenient to refer to this polyelectrolyte as XCPS.[1] The polymer has exceptionally high reduced viscosity, >5000 ml/g, which is relatively insensitive to temperature, ionic strength, shear, and pH. For this reason XCPS finds commercial use as a viscosity-enhancing agent for aqueous solutions. The solution conformation of this polysaccharide is the subject of the present manuscript.

The range of conformations available to polysaccharides and the principles which control interactions between polysaccharide chains are as yet poorly delineated in comparison with our detailed insight into polynucleotide and protein structure. The structure of ι-carrageenan, a sulfated galactan found in red seaweeds, may be taken as an example of the rich insights afforded only recently by modern methods: x-ray studies on ι-carrageenan fibers reveal a double helix (Arnott et al., 1974b); optical rotation, light scattering, and osmometry confirm the double helix in solution and demonstrate a thermally controlled helix–coil transition which is intimately related to the gelling of the polysaccharide (McKinnon et al., 1969; Rees et al., 1970; Jones et al., 1973).

The extracellular polymer of *Xanthomonas campestris*, which is the subject of the present report, was first isolated and characterized by Jeanes, Sloneker, and their co-workers (Jeanes et al., 1961; Sloneker and Jeanes, 1962; Sloneker and Orentas, 1962; Sloneker, Orentas, and Jeanes, 1964). The primary structure, recently reexamined by Jansson et al. (1975), is shown in Figure 1. It consists of a main chain of β-1,4-linked D-glucose units, as in cellulose, but with a three-sugar side chain attached to alternate glucose residues. The molecular weight of the native polymer is not clearly established; however, solutions prepared by heating the polymer for 3 h at 90 °C in 4 M urea yield a product showing a molecular weight of 1.4 to 3.6 $\times 10^6$ (Dintzis et al., 1970). Even under these conditions the intrinsic viscosity at zero shear remains high, i.e., 2900 ml/g.

The secondary and tertiary structures of this polymer are not known. However, viscosity–temperature profiles for the 0.5 to 1% dispersions of polymer revealed a sharp transition at 50–60 °C, in the absence of salt (Jeanes et al., 1961). In the presence of 0.1 to 1% KCl, no sharp transition was observed. A sharp decrease in optical rotation has also been reported for 1% dispersions at about 55 °C for the "no salt" case (Rees, 1972). These data suggest that the polymer possesses ordered secondary structure. We have extended these provocative earlier experiments to explore the polyelectrolyte nature of this polymer and to begin to learn its solution conformation, by carrying out three experiments. First we studied the effect of ionic strength on the titration of the carboxylate groups in the polymer. Second, we used optical rotation to examine the temperature-induced conformational transition in greater detail than previously reported. Third, we measured the changes in viscosity which accompany the conformational transition.

Experimental Section

The polysaccharide used was obtained from Kelco Company (Keltrol, no. 16573). This material contains cells and other undesired debris; CHN analysis shows 38% C, 5.5% H, and 1.2% N. This polymer was purified by a modification of the procedure of Jeanes et al. (1961). Polymer was dissolved to 0.3 g/l. in water and stirred overnight. NaCl (0.34 M) and EDTA (0.0025 M) were then added and the solution was mixed for 10 min at lowest speed with an Oster Model 847-01A blender. After adjusting the solution to pH 7, ethanol (300 ml/l. of H_2O) was added. The solution was degassed and centrifuged at 45 000 rpm for 90 min to remove cells, debris, and undispersed polymer. The supernatant S_1 was decanted and additional ethanol was added to S_1 (440 ml/l. of H_2O) to precipitate the polymer as a soft gel easily separated by centrifugation at 12 000 rpm for 30 min. The precipitate P_2 thus obtained was redissolved in water; EDTA and NaCl were added (0.0025 and 0.43 M, respectively).

The polymer was reprecipitated with ethanol (1 ml/ml of H_2O) and then again spun at 12 000 rpm for 30 min to isolate

[1] Abbreviations used: XCPS, the extracellular polymer produced by the bacterium *Xanthomonas campestris;* EDTA, ethylenediaminetetraacetic acid; PGA, poly(L-glutamic acid); PAA, poly(acrylic acid); CMC, carboxymethylcellulose.

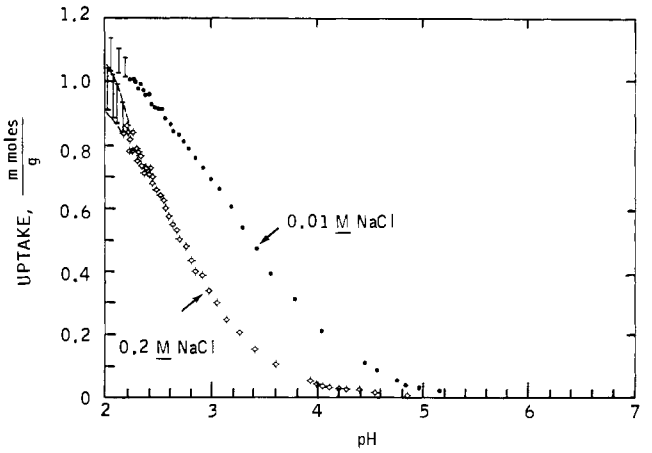

FIGURE 2: Hydrogen ion titration of XCPS polysaccharide, dissolved in 0.01 or 0.2 M NaCl. Polymer concentration, 2 mg/ml; titrant, 1 M HCl. Lyophilized polymer was used.

precipitate P_3. This material was redissolved in water and dialyzed exhaustively against redistilled deionized water at 5 °C. The "yield" was typically 60–70%. For most experiments this material was used immediately. However, for titration experiments (Figures 2 and 3) the polymer was lyophilized and redissolved as required. CHN analysis of this polymer reveals 39% C, 5.6% H, and 0.03% N (Kjeldahl). Measurement of the pyruvate content of the purified polymer by the method of Duckworth and Yaphe (1970) showed 2355 ± 110 g of XCPS per mol of pyruvic acid; i.e., 39% of the terminal mannose units of the side chain (Figure 1) bear a pyruvic acid acetal.

Chemicals were reagent grade used without further purification. Water was distilled, deionized, and redistilled. Glassware for experiments at low salt concentrations was carefully cleaned with alcoholic KOH and then rinsed in purified water.

Optical rotation was measured with a Jasco J-20 spectropolarimeter. Cells 10 cm long were used; an aluminum jacket controlled temperature through an external water bath. Temperature in the cell was monitored by the glass-sheathed platinum sensor of a Beckman T_m accessory. This accessory, plus a simple retransmitting potentiometer mounted in the Jasco, allowed direct, accurate recording of rotation vs. temperature data on an X–Y recorder.

pH was measured with a Radiometer PHM 26 meter. Potentiometric titrations were carried out with vigorous stirring on thoroughly degassed solutions under a nitrogen blanket. A micrometer syringe was used to add acid or base. Sodium and calcium ion activities were measured with Orion electrodes.

Viscosity at low shear was measured by a Brookfield Model LVF coaxial cylinder viscometer with UL adapter. The inner cylinder was Teflon-coated to prevent metal-ion contamination of solutions; a Lucite outer cylinder also allowed detection of bubbles. This instrument generates shear strains of 7.3 to 73 s^{-1}. Viscosity was also measured using a no. 75 Cannon-Ubbelohde four-bulb shear-dilution capillary viscometer. The bath temperature was 28 °C. The capillary viscometer is more precise than the Brookfield but generates higher shear strains.

Carbohydrate concentration was measured by the phenol–H_2SO_4 method (Dubois et al., 1956), using redistilled phenol. Glucose standards were routinely used; the optical density was read at 490 nm. The optical density generated by a given weight of glucose was 1.43 times the optical density of the same weight of purified and dried XCPS polymer.

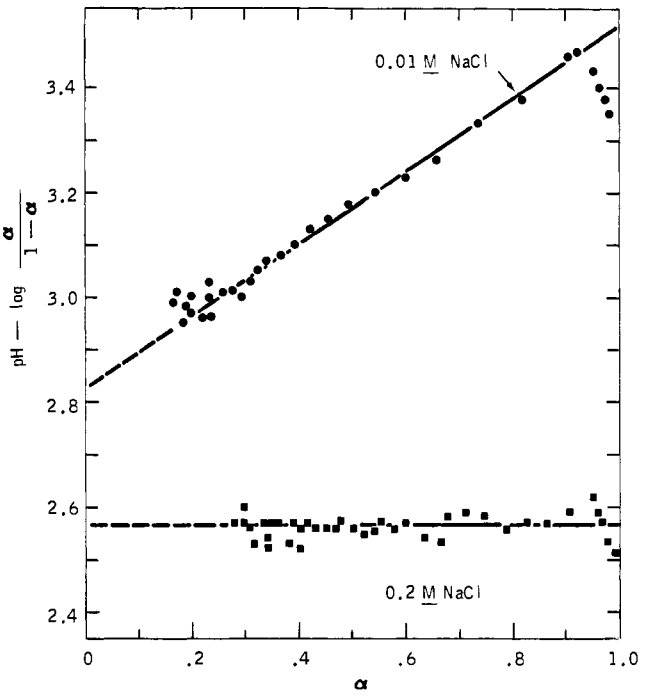

FIGURE 3: Replot of hydrogen ion titration data of Figure 2, according to the extended Henderson–Hasselbalch equation. The parameter α is the degree of dissociation of the carboxylic acid.

Results

The titration curve of a polyelectrolyte like XCPS is known to depend upon salt concentration and upon the distance between the acidic or basic groups. Figure 2 shows the uptake of acid by XCPS in the presence of 0.01 and 0.2 M NaCl. The data show a molecular weight of 830 ± 50 per mol of H^+ taken up; the potassium salt of the structure given in Figure 1 leads to a value of 639 per mol of H^+. Sloneker and Jeanes (1962) found equivalent weights of 675 and 764 for two batches of XCPS. Figure 2 shows that the apparent pK (midpoint of the titration curve) of the polymer is strongly influenced by the ionic strength. In 0.01 M NaCl, pK_{app} = 3.2, whereas in 0.2 M NaCl pK_{app} = 2.6.

It is informative (Tanford, 1961) to replot the data of Figure 2 according to the extended Henderson–Hasselbalch equation

$$pH - \log [\alpha/(1 - \alpha)] = pK_{int} + W\alpha$$

where W incorporates the interaction between COO^- groups and α is the degree of dissociation of the groups. This is done in Figure 3. It is apparent that at low salt the slope W is positive, indicating that the COO^- groups interact strongly. At high salt concentration, the slope is zero, which implies that each COO^- group acts independently; the interaction is shielded by a cloud of counterions. The intrinsic pK's are 2.8 in low salt, 2.6 at high salt. These values are on the lower end of the range typical for carboxylic polysaccharides (Rinaudo and Milas, 1974). The observed dependence of intrinsic pK on ionic strength is not unusual.

In order better to understand the temperature-induced conformational transition noted by viscosity and optical rotation measurements at high concentration (Jeanes et al., 1961; Rees, 1972), we studied the effect of monovalent and divalent cation concentration on the optical rotation at lower concentration, 0.06%. The results for NaCl and $CaCl_2$ are shown in the two frames of Figure 4. $MgCl_2$ acted similarly to $CaCl_2$. In all cases there is an abrupt change in rotation,

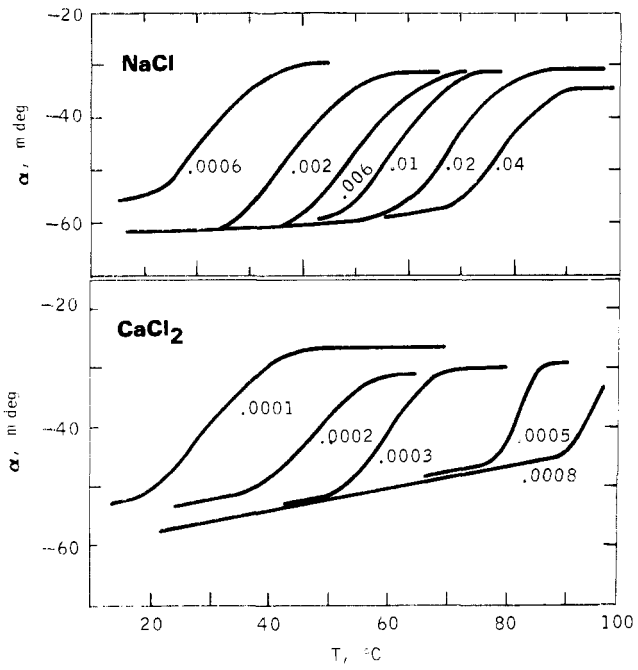

FIGURE 4: (Upper Frame) Optical rotation of XCPS solution (0.6 mg/ml) vs. temperature, in the presence of varying concentrations of NaCl. The NaCl concentration for each curve is indicated (0.0006 to 0.04 M). The pH is 7.0 ± 0.3. A 10-cm cell was used; the wavelength is 260 nm. (Lower Frame) Optical rotation vs. temperature in the presence of various $CaCl_2$ concentrations (0.0001 to 0.0008 M). All other conditions as in upper frame.

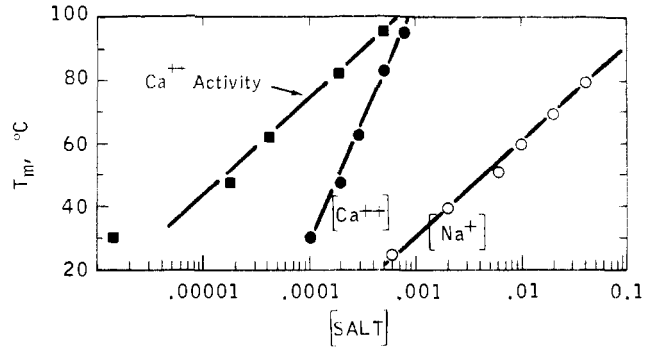

FIGURE 5: Melting temperature of XCPS as a function of counterion concentration and activity.

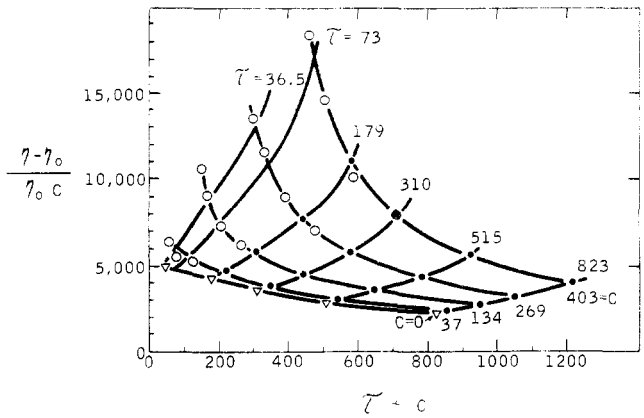

FIGURE 6: Reduced viscosity of XCPS vs. concentration and shear stress, at pH 7.0 in 0.27 M NaCl–0.014 M $CaCl_2$. The ordinate is $c + \tau$, where c is concentration in μg/ml and τ is shear stress in cP s^{-1}. Two viscometers were used. Open symbols were measured with Brookfield UL Couette viscometer. Filled symbols were measured with a capillary viscometer. The shear stress assigned to the capillary viscometry is that at the wall, corrected for non-Newtonian behavior.

suggestive of the thermal "melting" observed in DNA and proteins. The temperature at the midpoint of the transition is termed T_m. This transition temperature increases with increasing salt concentration for both Na^+ and Ca^{2+}. A comparison of the upper and lower frames of Figure 4 shows that Ca^{2+} is effective at much lower concentrations than Na^+, and that the transition breadth changes with Ca^{2+} concentration but is almost unaltered by Na^+ concentration.

The shapes of the individual rotation–temperature curves reveal that below T_m, in the low-temperature plateau region, the amplitude of the rotation diminishes gradually with temperature, suggesting a modest loosening of the native structure. Above T_m, a second plateau is reached in which the rotation is constant, suggesting a unique or statistically invariant denatured structure.

In Figure 5 T_m is plotted against the logarithm of the cation concentration for Na^+ and Ca^{2+} and for the cation activity of Ca^{2+}. (Sodium ion activity was almost identical with Na^+ concentration.) T_m changes by 30 °C per decade for Na^+ but changes by 70 °C per decade for Ca^{2+} concentration, and by 30 °C per decade for Ca^{2+} activity. A similar linear dependence of T_m on the logarithm of salt concentration is observed for DNA (Dove and Davidson, 1962; Schildkraut and Lifson, 1965).

The dependence of T_m on pH was also examined. For 0.01 M NaCl, lowering the pH from 7 to 4 causes T_m to increase by 15 °C. At pH 3.4 (degree of dissociation 0.5), T_m rises by more than 40 °C.

Is this thermally induced conformational change reversible? A solution that was heated with no added salt (T_m = 24 °C) and then quickly cooled retained the rotation of the denatured state. After 45 days at 5 °C, the rotation had returned halfway to its native value. However, if salt is added, either before heating or after quenching, the rotation quickly returns to the native value.

In order to obtain further insight into the structure of XCPS, the intrinsic viscosity and viscosity–temperature profiles of the polysaccharide were measured. The viscosity of XCPS is nonideal and non-Newtonian, even at high ionic strength (Jeanes et al., 1961). This is shown in Figure 6, in which data obtained with a four-speed rotating cylinder viscometer and a four-bulb capillary viscometer are plotted together. The ordinate in this figure is the reduced viscosity $(\eta - \eta_0)/\eta_0 c$. The abscissa, $c + \tau$, where c is the polysaccharide concentration and τ is the shear stress, combines concentration and shear-stress effects in a single plot. Four polymer concentrations, 37, 134, 269 and 430 μg/ml, were used in each viscometer. The shear stress assigned to the capillary viscometer data is that at the wall; the corresponding viscosity is corrected for non-Newtonian behavior by the Rabinowitsch method (Van Wazer et al., 1963).

In order to obtain the intrinsic viscosity of the polymer, the reduced viscosity data in Figure 6 should be extrapolated to zero concentration and zero shear stress. For this purpose, the viscosity data in Figure 6 are overlaid by two sets of curves: first, those interconnecting reduced viscosity values measured at constant concentration but differing shear stress; second, those interconnecting reduced viscosities obtained at constant shear stress but varying concentration. For the capillary viscometer the constant shear stress curves (τ = 179, 310, 515, and 823 cP s^{-1}) intersect the measured data points, but for the rotating cylinder viscosity data (τ = 36.5 and 73 cP s^{-1}) a

linear interpolation between the measured points was necessary.

Several features of the viscosity data are notable. First the reduced viscosity increases sharply with polymer concentration; the concentration dependence is most severe at low shear stress. Second, the reduced viscosity increases strongly with decreasing shear rate. However, the dependence of reduced viscosity on shear rate decreases as the concentration decreases. Third, for a given shear stress, the curves are easily extrapolated to zero concentration; the resultant curve for $c = 0$ is also shown in Figure 6. However, precise extrapolation to zero shear stress is not possible with the Brookfield rotating cylinder viscometer. We can only estimate the intrinsic viscosity at zero shear as 5000–7000 ml/g. This estimate must be regarded as a lower bound for the native polymer in the presence of substantial ionic strength because some degradation may have occurred in isolation or purification.

In order to illuminate the structural changes which must underlie the transition observed in the optical rotation studies, the viscosity of XCPS solutions was measured between 0 and 100 °C for the same range of salt concentrations used in the rotation studies. In Figure 7A are shown viscosity–temperature profiles for polymer concentration 0.6 mg/ml. The solutions used for the viscosity studies gave well-defined transitions in optical rotation before and after the viscosity experiment.

A sharp, salt-dependent transition is not obvious in the reduced viscosity–temperature curves at this low concentration. However, the viscosity change with temperature appears to show two characteristic segments. At low temperature the reduced viscosity gradually increases with temperature, rises to a peak, and then slowly falls. Above T_m, the dependence on T changes in character. For high salt concentration, a sharp drop in slope occurs at T_m, whereas at low salt concentration the decrease is less, and at "no salt" the two characteristic segments blend smoothly together, so that no "melting" is detectable. The data suggest that below T_m the molecules are in a relatively salt-independent conformation. The gradual increase in η_{red} with temperature, below T_m, could arise from excluded volume effects rather than structural perturbations. Above T_m, a more salt-sensitive structure occurs. For low salt, the reduced viscosity actually increases, suggesting that a more extended conformation is generated by repulsion among COO^- groups. At higher salt concentrations, the reduced viscosity decreases at high temperature, indicating a collapsed structure.

This interpretation of the viscosity–temperature profiles in Figure 7A is supported by viscosity–temperature measurements at slightly higher concentration, 1.65 mg/ml, which are shown in Figure 7B. This concentration is still well below the concentrations at which gelation occurs, but high enough to present a somewhat clearer pattern. At 1.65 mg/ml, when no salt is added, no sharp transition in viscosity occurs at T_m. However, at higher salt concentrations T_m correlates with a well-defined change in the slope of the viscosity–temperature curve.

The results presented in Figure 7 are in accord with low-concentration studies of Jeanes et al. (1961). At much higher concentrations, 10 mg/ml, they found a sharp transition in η at 50–60 °C, in the absence of added salt. We verified Jeanes' observation. When this occurred, the rotation was very large, and of erratic sign, at low temperatures. These observations suggest that the low temperature form is a gel at higher concentrations. Two transitions in rotation then occurred, the first to rotation values consistent with those in dilute solution, the second, at higher temperatures, like those reported in Figure 4. The sharp increase in viscosity reported by Jeanes et al. (1961) seemed to coincide with the latter process.

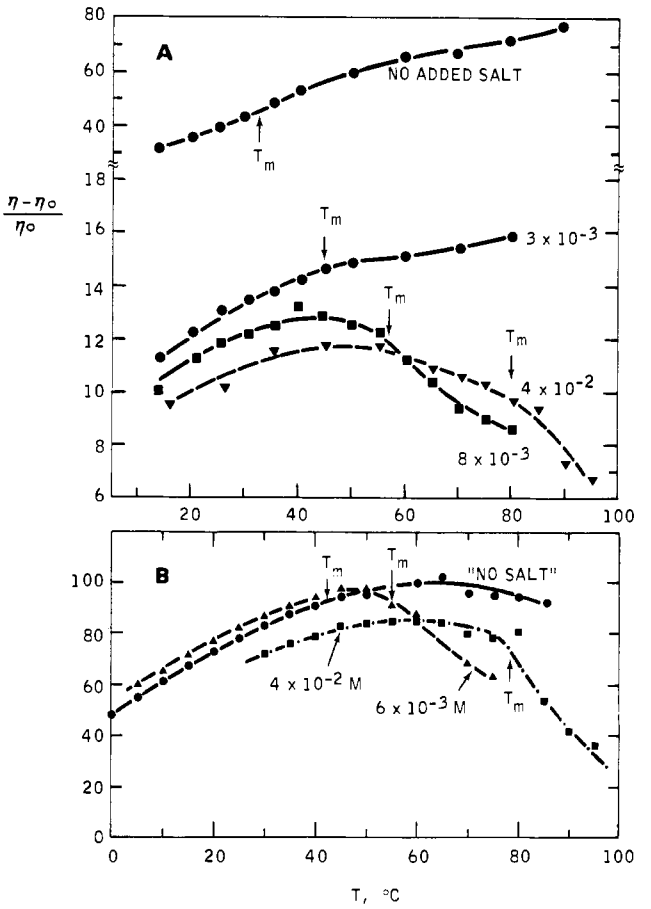

FIGURE 7: (A) Specific viscosity of XCPS solution, 0.6 mg/ml, pH 7.0 ± 0.3, vs. temperature, at four different NaCl concentrations. (B) Specific viscosity of XCPS solutions, 1.65 mg/ml, pH 7.0 ± 0.3, vs. temperature, at three different NaCl concentrations. The molarity of NaCl for each curve is indicated. The melting temperature, measured by optical rotation, is marked by an arrow for each curve. A Brookfield LVF-UL Couette viscometer was used.

Discussion

The titration experiments show that native XCPS behaves as a typical polyelectrolyte (Tanford, 1961; Nagasawa, 1971; Katchalsky, 1971) with moderately strong interaction between the COO^- groups. For XCPS the difference between pK_0 and pK_{app} at 0.01 M NaCl is 0.4 to 0.6, at a polymer concentration of 2 g/l. (0.003 M in pentamer repeat units). Titration at infinite dilution might increase the difference between pK_0 and pK_{app} by at most 0.1 (see data for polyacrylic acid in Nagasawa et al., 1965).

Do these data limit the possible secondary structure of XCPS? Consider the titration behavior of several polyelectrolytes of known structure. Table I lists $pK_{app} - pK_0$ and b, the distance between COO^- groups, as projected on the molecular axis, for three polymers: α-helical poly(L-glutamic acid) (PGA), poly(acrylic acid) (PAA), and carboxymethylcellulose (CMC). From such data one may *crudely* estimate the distance between COO^- groups in XCPS from the following relations (Manning and Holtzer, 1973).

$$\mathrm{pH} - \log \frac{\alpha}{1-\alpha} = pK_0 - g(\alpha) \log \kappa^2 a^2$$

where κ^{-1} is the usual Debye–Huckel radius, a is the poly-

TABLE I: Titration Behavior of Polyelectrolytes.[a]

Polymer	$pK_{app} - pK_0^b$	b (Å)	Structure Used to Estimate b
PGA, helical	1.9	1.52	α helix
PAA	1.8	2.5	Fully extended chain
CMC	1.3	3.4	Cellulose I structure, single stranded
XCPS	0.6	9.2 (?)	Cellulose I structure, single stranded; degree of pyruvate substitution = 0.13

[a] References for data: PGA, extrapolation of curves reported by McDiarmid and Doty (1966); PAA and CMC, Nagasawa (1971). The degree of esterification of the CMC is 1.54. [b] In 0.01 M salt.

electrolyte cylinder radius, and $g(\alpha)$ is a parameter describing the charge per unit length of the polymer at a given value of α. The function $g(\alpha)$ varies inversely as the distance b. If one assumes that the cylinder radius a and intercharge dielectric constant for single-stranded XCPS and CMC are identical, then one would predict $\Delta pK = 0.48$ for XCPS. This is only slightly less than the observed value. If the cylinder radius and dielectric constant are larger for XCPS, as seems highly likely because the charged groups are in the three-sugar side chain, then the observed ΔpK of XCPS would require multistrand structures or a single-strand structure more compact than that of CMC. The former seems more probable from known structures of agarose and carrageenans. A more precise measure of b for XCPS may be obtainable from measurements of counterion activity in a titration experiment (Rix-Montel et al., 1974).

The increase in transition temperature with increasing salt concentration, as seen in the optical rotation data (Figure 4), shows that the native conformation is destabilized by repulsion among the COO^- groups. This destabilization can be muted by added salt. The denatured conformation must then be one in which the COO^- groups are further apart than in the native form. DNA shows similar behavior due to repulsion between phosphate groups. The experimentally established value of b for DNA changes from 1.7 Å in the native B form to 4.1–4.7 Å in the thermally denatured form (Rix-Montel et al., 1974; Record, 1975).

It was noted above that the transition breadth for XCPS is relatively independent of Na^+ concentration but increases greatly at low Ca^{2+} concentration. The effect of Na^+ and Mg^{2+} concentrations on the transition breadth of DNA shows a similar pattern (Dove and Davidson, 1962; Record, 1975).

The linear dependence of T_m on the logarithm of the counterion activity seen here for XCPS (Figure 5) has been observed also for DNA (Dove and Davidson, 1962, Schildkraut and Lifson, 1965) and is the expected behavior for rodlike polyelectrolytes. The molecular mechanism for the effect of salt on melting temperature in DNA is now well understood (Privalov et al., 1969; Manning, 1972a,b). Briefly, these studies show that the transition enthalpy is independent of salt concentration, but the transition entropy difference between native and denatured conformations, in the presence of excess salt, contains two salt-dependent terms. The first arises from differences in the entropy of mixing of the uncondensed counterions with solvent counterions for the two conformations. The second arises from differences in free energy originating in the interaction of unneutralized acid groups with their surrounding Debye-Huckel atmospheres. The first term makes the helix more stable in the presence of salt while the second mechanism destabilizes the helix in the presence of more salt. Both give logarithmic dependence of T_m on salt. In the case of DNA, and in the case of XCPS, the first effect appears to dominate. (We note in passing that Manning's theory is valid only in the presence of excess salt. There is excess salt for the Na^+ data but not for the Ca^{2+} results in Figure 4.)

The absence of a sharp change in η at T_m distinguishes XCPS from DNA and from globular proteins. The viscosity data suggest that the native and denatured states of XCPS have similar anisometry. The denatured form appears to derive its anisometry in part from repulsion among the negatively charged groups since the viscosity of the denatured form decreases sharply with added salt. The native molecule is less responsive to added salt; this suggests that its anisometry originates in hydrogen bonds, in steric limitations of dihedral angles, or in other charge-insensitive interactions.

The marked dependence of renaturation rate of XCPS on ionic environment recalls a similar dependence in polynucleotides; the rate of polynucleotide double-helix formation from single-stranded chains increases by several powers of ten with the addition of salt (Ross and Sturtevant, 1960; Studier, 1969). Double-helical structures have been observed in fibers of polysaccharides such as agarose and carrageenan (Arnott et al., 1974a,b), and in carrageenan solutions (Jones et al., 1973). Do similar structures exist in XCPS? Our results are not conclusive. The optical rotation data suggest a conformational change which might involve multistrand helix breakdown, but could also involve reorientation within a single-stranded structure of the three-sugar side chain bearing the COO^- groups. The viscosity–temperature data provide no insight. Further experiments will be required to establish the number of strands in native and denatured XCPS.

Acknowledgment

The experiments reported here were carried out with the expert technical assistance of Miss Jacqueline Ogletree. Stimulating discussions with A. I. Laskin and L. Naslund are also gratefully acknowledged.

References

Arnott, S., Fulmer, A., Scott, W. E., Dea, I. C. M., Moorhouse, R., and Rees, D. A. (1974a), *J. Mol. Biol. 90,* 269–284.

Arnott, S., Scott, W. E., Rees, D. A., and McNab, C. G. A. (1974b), *J. Mol. Biol. 90,* 253–267.

Dintzis, F. R., Babcock, G. E., and Tobin, R. (1970), *Carbohydr. Res.,* 257–267.

Dove, W. F., and Davidson, N. (1962), *J. Mol. Biol. 5,* 467–478.

Dubois, M., Gilles, K. A., Hamilton, J. K., Rebers, P. A., and Smith, F. (1956), *Anal. Chem. 28,* 350–356.

Duckworth, M., and Yaphe, W. (1970), *Chem. Ind. (London) 13,* 747–748.

Eigner, J., and Doty, P. (1965), *J. Mol. Biol. 12,* 549.

Jansson, P. E., Kenne, L., and Lindberg, B. (1975), *Carbohydr. Res. 45,* 275–282.

Jeanes, A., Pittsley, J. E., and Senti, F. R. (1961), *J. Appl. Polym. Sci. 5,* 519–526.

Jones, R. A., Staples, E. J., and Penman, A. (1973), *J. Chem. Soc., Perkins Trans. 2,* 1608–1612.

Katchalsky, A. (1971), *Pure Appl. Chem. 26,* 327–373.

McKinnon, A. A., Rees, D. A., and Williamson, F. B. (1969), *J. Chem. Soc., Chem. Commun.,* 701–703.

Manning, G. S. (1972a), *Biopolymers 11,* 937–949.

Manning, G. S. (1972b), *Biopolymers 11,* 951–955.

Manning, G. S., and Holtzer, A. (1973), *J. Phys. Chem. 77,* 2206–2212.
McDiarmid, R., and Doty, P. (1966), *J. Phys. Chem. 70,* 2620.
Nagasawa, M. (1971), *Pure Appl. Chem. 26,* 519–536.
Nagasawa, M., Murase, T., and Kondo, K. (1965), *J. Phys. Chem. 69,* 4005–4012.
Privalov, P. L., Ptitsyn, O. B., and Birshtein, T. M. (1969), *Biopolymers 8,* 559–571.
Record, M. T., Jr. (1975), *Biopolymers 14,* 2137–2158.
Rees, D. A. (1972), *Biochem. J. 126,* 257–273.
Rees, D. A., Scott, W. E., and Williamson, F. B. (1970), *Nature (London) 227,* 261.
Rinaudo, M., and Milas, M. (1974), *J. Polym. Sci., Polym. Chem. Ed. 12,* 2073–2081.
Rix-Montel, M. A., Grassi, H., and Vasilesc, D. (1974), *Biophys. Chem. 2,* 278–289.
Ross, P. D., and Sturtevant, J. M. (1960), *Proc. Natl. Acad. Sci. U.S.A. 46,* 1360–1365.
Schildkraut, C., and Lifson, S. (1965), *Biopolymers 3,* 195.
Sloneker, J. H., and Jeanes, A. (1962), *Can. J. Chem. 40,* 2066–2071.
Sloneker, J. H., Orentas, D. G., and Jeanes, A. (1964), *Can. J. Chem. 42,* 1261–1269.
Studier, F. W. (1969), *J. Mol. Biol. 41,* 199–209.
Sutton, J. C., and Williams, P. H. (1970), *Can. J. Bot. 48,* 645–651.
Tanford, C. (1961), Physical Chemistry of Macromolecules, New York, N.Y., Wiley.
Van Wazer, J. R., Lyons, J. W., Kim, K. Y., and Colwell, R. E. (1963), Viscosity and Flow Measurement, New York, N.Y., Wiley.

Binding of Platinum and Palladium Metallointercalation Reagents and Antitumor Drugs to Closed and Open DNAs†

Mary Howe-Grant, Kun C. Wu, William R. Bauer,* and Stephen J. Lippard*

ABSTRACT: The interaction of platinum and palladium complexes with closed and nicked circular and linear DNAs was investigated by a variety of methods. Cationic metal complexes containing flat, aromatic ligands, such as 2,2′,2″-terpyridine, *o*-phenanthroline, and 2,2′-bipyridine, interfere with the usual fluorescence enhancement of ethidium bromide by competing for intercalation sites on calf-thymus DNA. Metal complexes having kinetically exchangable ligands, including the antitumor drugs *cis*-$[(NH_3)_2PtCl_2]$ and $[(en)PtCl_2]$, inhibit noncompetitively the DNA-associated ethidium fluorescence enhancement by binding covalently to the bases and blocking potential intercalation sites. Only the metallointercalators were capable of altering the DNA duplex winding, as judged by the effects of these reagents upon the electrophoretic mobility and sedimentation behavior of PM-2 DNAs. Long-term ($t > 120$ h) interactions of metal complexes with PM-2 DNAs I, I_0, and II, corresponding to superhelical, closed relaxed, and nicked circles, respectively, showed that covalent binding occurs the most readily to DNA I, possibly because of the presence of underwound duplex regions in this tightly wound superhelical DNA. The active antitumor drugs *cis*-$[(NH_3)_2PtCl_2]$ and $[(en)PtCl_2]$ bind covalently to DNA I under conditions where the inactive *trans*-$[(NH_3)_2PtCl_2]$ does not. Most of the complexes studied were capable of producing chain scissions in PM-2 DNA I. Exceptions are the kinetically inert complexes $[(bipy)Pt(en)]^{2+}$ and $[(terpy)Pt(SCH_2CH_2OH)]^+$, suggesting that covalent binding might be a prerequisite for nicking.

Recent studies in our laboratories have demonstrated that the $[(terpy^1)Pt(HET)]^+$ monocation (Figure 1) binds to double-stranded DNAs by intercalation with a duplex unwinding angle comparable to that of ethidium bromide (EtdBr) (Jennette et al., 1974). The electron-dense platinum atoms in this complex, intercalatively bound to calf-thymus DNA, were subsequently detected by fiber x-ray diffraction techniques at a distribution along the helix axis that accords with the nearest neighbor exclusion binding model (Bond et al., 1975). The present study was undertaken to determine the effects of charge, number of aromatic ligands, number of chelate rings, and choice of additional ligands on the intercalative binding of metallointercalation reagents to DNA. Moreover, since it has been suggested (Thomson et al., 1972) that the mechanism of action of the platinum antitumor drugs (Rosenberg and Van Camp, 1970; Cleare, 1974) might involve intercalative binding to DNA, several compounds in this class were included in the investigation.

We have also examined the nature of the nonintercalative interaction of several metal complexes with DNA by monitoring the changes in electrophoretic mobility of both closed and nicked circular PM-2 DNAs that had been incubated with reagent. A growing body of evidence has suggested that the

† From the Department of Chemistry, Columbia University, New York, New York 10027 (M.H-G. and S.J.L.), and the Department of Microbiology, Health Sciences Center, State University of New York, Stony Brook, New York 11794 (K.C.W. and W.R.B.). *Received April 23, 1976.* This work was supported by United States Public Health Service Grants CA-15826 (to S.J.L.) and GM-21176 (to W.R.B.), and by a National Institutes of Health National Research Service Award (to M.H-G.), Training Grant No. GM-07216.

[1] Abbreviations are: EtdBr, ethidium bromide; r_f, formal ratio of metal to nucleotide concentrations; Tris, tris(hydroxymethyl)aminomethane; EDTA, disodium salt of ethylenediaminetetraacetic acid; $^{24}\sigma_0$, number of superhelical turns per ten base pairs in a native closed DNA, assuming an EtdBr unwinding angle of 24°; terpy, 2,2′,2″-terpyridine; bipy, 2,2′-bipyridine; *o*-phen, *ortho*-phenanthroline; en, ethylenediamine; dien, diethylenetriamine; HET, 2-hydroxyethanethiolato; AET, 2-aminoethanethiolato; CMT, carboethoxymethanethiolato; and cys, cysteinato; uv, ultraviolet.